NANO LETTERS

2007
Vol. 7, No. 8
2535−2539

Electrodeposited Bismuth Telluride Nanowire Arrays with Uniform Growth Fronts

Lynn Trahey, Catherine R. Becker, and Angelica M. Stacy*

Department of Chemistry, University of California, Berkeley, California 94720

Received March 26, 2007; Revised Manuscript Received May 24, 2007

ABSTRACT

Bismuth telluride (Bi_2Te_3) nanowires were deposited into porous alumina templates with 35 nm diameter pores by a pulsed-potential electrodeposition method. For growth at temperatures between 1 and 4 °C, the nanowires filled 93% of the pores of the template, and the growth fronts were uniform with nanowire lengths of ~62–68 μm. There are over ten billion nanowires per square centimeter with aspect ratios approaching 2000:1. Samples were characterized by scanning and transmission electron microscopy, X-ray diffraction, and electron microprobe analysis. The crystalline nanowire arrays are highly oriented in the [110] direction, which is optimal for thermoelectric applications.

The synthesis of dense, conductive nanowire arrays is critical for ultimately realizing the potential benefits of nanowire components in electronic devices. One of the leading ways of fabricating nanowire arrays is electrodeposition of materials into templates.[1−3] A challenge of this method is growing the wires at even growth rates, so that the nanowires fill the pores to a uniform length. Uniform nanowire lengths will allow for contacting the largest number of wires possible in an electronic device, leading to maximum device performance.

The templated electrodeposition of nanostructures has been in development since the late 1960s.[4] In this Letter, we report a pulsed-potential deposition technique for the synthesis of highly ordered bismuth telluride (Bi_2Te_3) nanowire arrays. Doped Bi_2Te_3 is a well-known thermoelectric (TE) material used for refrigeration.[5,6] Electrodeposition of Bi_2Te_3 nanowires has been widely studied[7−12] because of predictions of enhanced TE performance with confined dimensions.[13,14] Our templated pulsed-potential electrodeposition process is unique for producing uniform nanowire growth lengths for over ten billion nanowires per square centimeter in pores with aspect ratios of 2000:1.

Electrodepositing a material that forms as favorably as Bi_2Te_3 at a single deposition potential or current density often yields arrays that do not fill all of the pores in the template due to the overgrowth of select wires. Overgrowth is characterized by the formation of a thin film of the material that covers the pores of the template. This occurs because a few wires reach the top of the template first and then grow laterally. The film blocks the unfilled channels from the solution and prohibits the nanowire growth therein. The keys to preventing premature overgrowth of nanowires are 2-fold: (1) employing pristine, reproducibly made templates with a narrow pore-diameter distribution and straight, unbranched pores and (2) nucleating and growing the nanowires at uniform rates. To reach these goals, our current process utilizes highly ordered, homemade porous alumina templates and a pulsed-potential deposition technique.

Porous anodic alumina (PAA) is a common choice for a nanowire template[3,15] because it is electrically insulating, reasonably robust, has a high number of pores per unit area and its dimensions can be tailored to meet the desired nanowire specifications. Since the reproducibility and quality of the nanowire template are critical to the reproducibility of nanowire electrodepositions, commercially available templates sold as filters are not acceptable because they exhibit large variations in pore diameter and the pores are highly branched. PAA templates were produced in a manner similar to that reported previously[16] but with the addition of a two-step anodization process that greatly increases the uniformity of the nanoporous array[17] (see Supporting Information for more detail). Templates used were routinely 70 μm (±0.05 μm) thick with 35 nm (±1 nm) pore diameters at the surface and over 10 billion pores per square centimeter as determined from scanning electron microscope (SEM) images.

The PAA templates were incorporated into three-electrode cells, described previously,[18] for the electrodeposition of Bi_2Te_3. Metal layers consisting of 500 nm platinum films on a wetting layer of titanium were sputtered onto one side of the PAA template to serve as the working electrode (Thin Film Technology, Inc.). The Ti wetting layer covered only the alumina, allowing the deposition to be initiated on the

* Corresponding author. E-mail: Astacy@berkeley.edu.

10.1021/nl070711w CCC: $37.00
Published on Web 07/13/2007

sputtered Pt. Copper disks were attached to the metal layer on the PAA template with silver paste and soldered to a copper wire. All exposed copper and solder were masked with clear nail polish so that the working electrode surface was limited to the Pt layer at the bottom of each pore. The area of exposed template in solution was roughly 2 cm^2. The deposition cells were chilled using a cold plate (Blackcat SK-12) that held 1 M nitric acid solutions containing dissolved bismuth (7.5×10^{-3} M) and tellurium (0.01 M) at the desired deposition temperatures (1−10 °C). The applied voltage and the resulting current data were collected with a data acquisition system (Agilent 34970A).

The deposition potentials for Bi_2Te_3 were selected from cyclic voltammograms (CVs). For more negative deposition potentials, the composition of the binary compound shifts from Bi_2Te_3 to more Bi-rich phases (Bi_4Te_5, Bi_6Te_7).[12] It was expected that more positive values would also result in the formation of Bi_2Te_3, but at slower rates. Therefore, −420 mV vs Hg/Hg_2SO_4 (saturated K_2SO_4) was chosen. The "rest" potential of −300 mV for the pulse potential deposition was selected from a region of the CV where there is no appreciable current, between the reduction and oxidation potentials of the compound. For the pulse regime reported, the reduction potential was applied for 1 s, followed by 2 s of the "rest" potential, with a 1 V/s scan rate between them. Depositions were stopped when the first spot of gray overgrowth was observed visually at the template edge, indicating that some wires had reached the top of the template. After each deposition, the samples were released from the working electrode assembly with acetone.

SEM (Hitachi S-5000) was used to study the growth rate, nucleation percentage, and morphology of the nanowire arrays. SEM samples were prepared from regions near the center of the templates and are representative of the majority of the total template area. Samples were sputtered with approximately 1 nm of iridium (Baltec MED 010) before imaging. All images reported were taken with backscattered detection at an operating voltage of 10 kV. Plan-viewed samples were polished with 1 μm diamond paste followed by 0.05 μm colloidal silica before analysis when necessary.

SEM micrographs of template cross sections reveal that Bi_2Te_3 nanowire arrays exhibit very high wire densities at the top (outer surface) of the templates (Figure 1a). When produced at low temperatures (1−4 °C), the nanowires fill about 93% of the length of each pore, which is made possible due to the narrow wire-length distribution that the array exhibits (Figure 1b). This uniform growth front corresponds to a growth rate of roughly 2.7 μm/h, and wires that range between ∼62 and 68 μm long in the 70 μm thick template. The growth rate increased to about 5.5 μm/h when the deposition solution was not chilled. In samples deposited at above 10 °C, the growth front appears to have two distinct lengths (parts c and d of Figure 1). The double growth front was even more pronounced when the reduction potentials were more negative (−430, −450, −475 mV). Since a double growth front is not observed near 1 °C, we attribute this feature to the increased growth rate at higher temperatures and/or nonuniform nanowire nucleation rates. This feature exists from a very early stage of growth and increases in wire-length disparity as the deposition progresses.

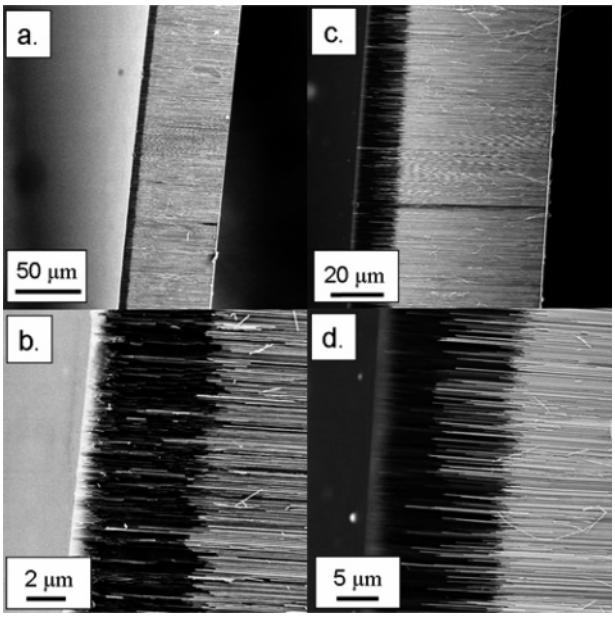

Figure 1. Back-scattered SEM images of Bi_2Te_3 nanowire array cross sections in which the bright horizontal lines are the nanowires and the darker areas are the PAA templates (70 μm thick). (a) Low-temperature (1−4 °C) full cross section with the working electrode on the far right side. Nanowires grew from right to left. (b) Closeup of low-temperature array nanowire growth front. (c) Room-temperature (22−23 °C) full cross section. Nanowires again grew from right to left. (d) Closeup of room-temperature array nanowire growth front.

The wire nucleation percentage was determined by mechanically polishing the Pt layer at the bottom of the template to expose the base of the array. SEM images show that the wires grown at all temperatures studied nucleate in an estimated 95% of the pores (Figure 2a). This result is 15% higher than what we had achieved for direct potentiostatic depositions[18] and is attributed to the measures taken to ensure that the pores are uniform and identical to one another, as well as to the pulsing of the potential.

A template produced at 1−2 °C was allowed to overgrow, and the overgrowth subsequently was polished off to determine the percentage of wires that reached to within 2 μm of the top of the template. As shown in Figure 2b, over 70% of the nucleated wires reached the outer edge of the template before nanowire overgrowth. We expect that if the samples were polished down to 10 μm from the outer edge, at least 95% of the nucleated wires would be exposed. Our goal, however, is to produce dense arrays that do not overgrow the templates to avoid the need for mechanical polishing, as this will likely lead to microscopic cracks in the nanowires that may hinder the performance of the array in a device.

In a diffusion-limited direct deposition, the pore channels in which wires nucleate first will be favored as the deposition progresses because those nanowires are closer to the bulk solution. Pulsing the deposition potential improves the nanowire length uniformity by significantly slowing the nanowire growth rate across the entire array. Special attention should first be given to the uniformity of the porous alumina

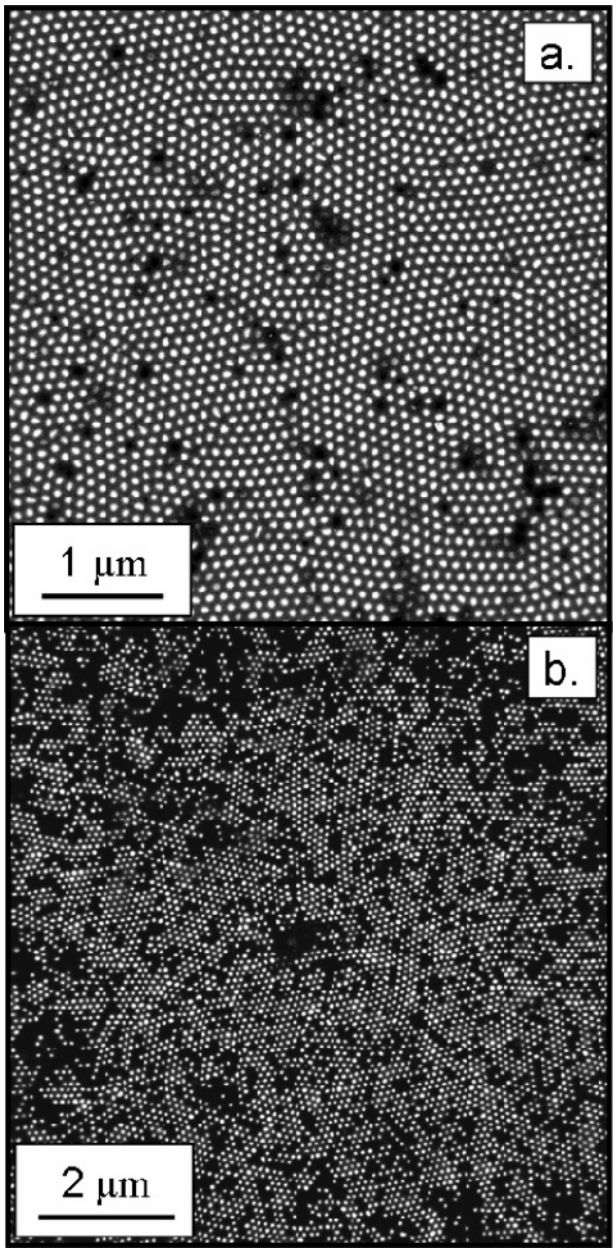

Figure 2. Plan-view SEM images of nanowire array composites. Bright dots are nanowires. (a) Room-temperature grown array with the working electrode polished away to reveal the nucleation percentage of the nanowires. (b) Low-temperature grown array with the overgrowth polished back to reveal the number of wires that reached to within 2 μm of the template's top (outer) surface.

template and quality of electrode. Then, reducing the cationic species for only a fraction of the total deposition time allows ions to re-equilibrate near the nanowire surfaces for the remaining time, regulating nanowire growth.

X-ray diffraction patterns (Siemens D5000 Powder Diffractometer, Cu Kα radiation) of arrays grown at different temperatures are shown in Figure 3. In order to probe the orientation of the nanowires, care was taken to choose X-ray diffraction (XRD) samples with no overgrowth. The 110 reflections are significantly enhanced indicating strong texturing, similar to what we have seen in the past.[16,18,19] The broad alumina peak at ~23° (2θ) is no longer evident because it is obscured by the large quantity of Bi_2Te_3 present.

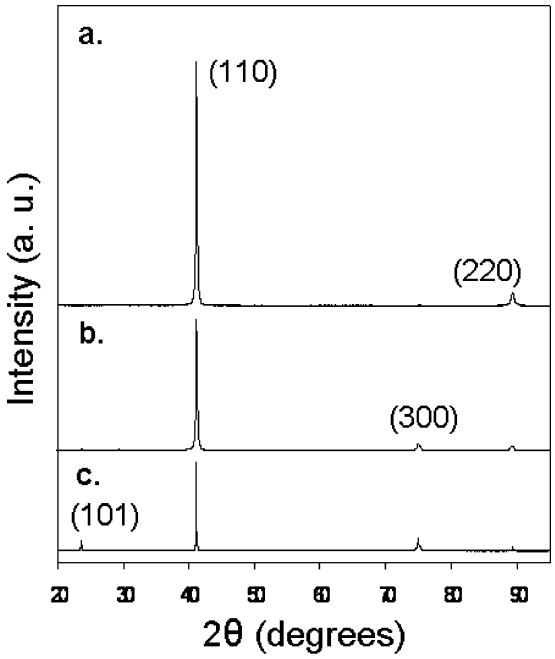

Figure 3. Representative X-ray diffraction patterns of not-overgrown Bi_2Te_3 nanowire arrays produced at (a) 1−4 °C, (b) 7−10 °C, and (c) room temperature (22−23 °C). The peaks match to well-known powder pattern peaks for Bi_2Te_3 (Powder Diffraction Files 82-0358, 15-0863).

Preferred orientation along the [110] direction is advantageous for TE applications[5] and is different from the preferred orientation produced from other pulsed-potential depositions.[8]

The 300 peak is present in addition to the 110 reflection for arrays grown at mid-temperatures (7−10 °C), as shown in Figure 3b. For room-temperature (22−23 °C) depositions, the 101 peak is also present (Figure 3c). We attribute the additional peaks in the mid-temperature and room-temperature diffraction patterns to faster nanowire growth rates. Wires grown slowly at low temperatures are highly oriented with the layers of the compound aligned parallel to the growth axis. Misalignments in the preferred orientation are induced when the wires are forced to grow faster by depositing at higher temperature. The double growth front observed in some arrays may be due to select wires with one orientation growing faster than wires with a different orientation.

The composition of a Bi_2Te_3 array produced at 1−2 °C was analyzed using electron microprobe analysis (EPMA, Cameca SX-51) calibrated with Al_2O_3, Bi (metal), and ZnTe. To prepare the sample, the backing electrode was mechanically polished off to provide a flat surface for analysis. An overall Bi:Te ratio of 0.54:1 is observed, instead of the 0.67 expected for Bi_2Te_3. This value is consistent over the entire nanowire array. According to the Bi/Te phase diagram,[20] there are no known Bi/Te binary phases that are more Te rich than the 2:3 phase. This suggests that excess Te is present as a second phase. Since elemental Te is not detected in the XRD patterns, we postulate that Te has been incorporated at grain boundaries in the compound or at the nanowire−alumina interface.

A possible explanation for the excess Te in the nanowires was found by analyzing the current data recorded during the

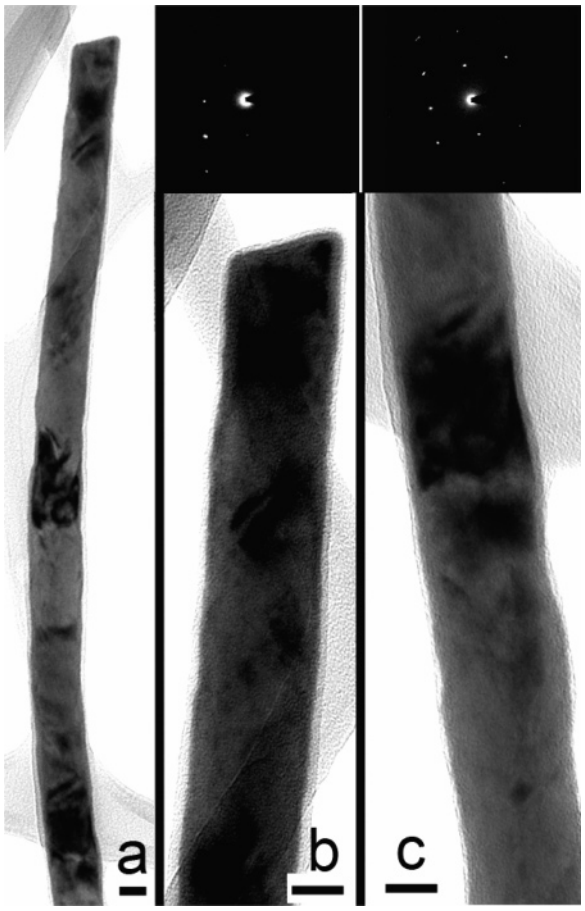

Figure 4. Bright field TEM micrographs of a released nanowire, with corresponding diffraction patterns at two locations along the wire length. Images b and c are from the upper and lower edges of a, respectively. The mottled contrast in the dark areas along the wire length is due to bend contours interacting with localized strained fields. The slight curvature of the nanowire results in a 10° rotation in the diffraction patterns. Scale bars represent 20 nm.

pulsed-potential experiments. It was observed that at the "rest" potential, positive (oxidation) currents were recorded throughout the depositions. It is known from the CV of this system[12] that Bi_2Te_3 oxidizes first to Bi^{3+} and Te^0 on the anodic wave of the CV. More positive potentials are required to oxidize Te^0. This suggests that at the "rest" potential chosen, Bi is removed from the nanowires selectively, leaving Te deposited. Preferentially stripping Bi from Bi_2Te_3 at the "rest" potential may account for the low Bi:Te ratio determined through microprobe analysis. It would be optimal to have no current during the time when channels are refilling with cations. A slightly more negative rest potential or the creation of an on/off potential cycle could address this problem.

Recently, it was reported that pulsed-potential deposition produces single-crystalline Bi_2Te_3 nanowires.[8] Our synthesis conditions produce highly oriented, crystalline wires with localized strain gradients. Transmission electron microscopy (TEM, Philips Tecnai 12) was used to analyze the microstructure of nanowires deposited at low temperature. The wires were released by dissolving the PAA template in 1 M NaOH for approximately 1 h, followed by rinsing with water and isopropyl alcohol. Bright field micrographs of a representative wire with corresponding diffraction patterns from two locations along the wire length are shown in Figure 4. The mottled contrast along the wire length is indicative of localized strain fields. The origin of this strain is still under investigation, though it is suspected to be due to compositional gradients.

A uniform nanowire array growth front will allow for maximum electrical contact to the wires, which will lead to quantifiable nanowire property measurements and optimal thermoelectric device performance. The integration of pulsed-potential deposition into the synthesis of Bi_2Te_3 nanowires has helped us achieve incredibly dense arrays of nanowires with aspect ratios approaching 2000:1 due to the uniformity in which the nanowires nucleate and grow in relation to their neighbors. The Bi_2Te_3 wires are highly oriented with the {110} planes parallel to the wire axis when grown at low temperatures, but the orientation is shifted off this axis by increasing the nanowire growth rate. With the combined factors of uniform PAA templates and support of cation diffusion, PAA templates have been filled with Bi_2Te_3 nanowires to an extent never before reported.

Acknowledgment. The authors thank the Office of Naval Research (Contract No. N00014-01-1-1058), Lockheed Martin (Contract No. XVX458640E), and NASA GSRP (Contract Nos. NGT-1-03009 and NGT-1-03003) for funding. We also thank Dr. Jeff Sharp (II−VI Semiconductors), Professor Ron Gronsky (UC Berkeley), and Dr. Graham Yelton (Sandia National Labs) for helpful discussions. Last, we thank UC Berkeley's Electron Microscope Lab for use of the SEM, Nanosys Inc. for use of the TEM, and Kent Ross (UC Berkeley) for EPMA services.

Supporting Information Available: Experimental procedure for fabrication of porous alumina templates used in these experiments. This material is available free of charge via the Internet at http://pubs.acs.org.

References

(1) Aranda, P.; Garcia, J. M. *J. Magn. Magn. Mater.* **2002**, *249*, 214−219.
(2) Bera, D.; Kuiry, S. C.; Seal, S. *JOM* **2004**, *56*, 49−53.
(3) Shingubara, S. *J. Nanopart. Res.* **2003**, *5*, 17−30.
(4) Possin, G. E. *Rev. Sci. Instrum.* **1970**, *41*, 772−774.
(5) Goldsmid, H. J. *Electronic Refrigeration*; Pion Limited: London, 1986.
(6) Nolas, G. S.; Sharp, J.; Goldsmid, H. J. *Thermoelectrics: Basic Principles and New Materials Developments*; Springer: Berlin, 2001.
(7) Jin, C. G.; Xiang, X. Q.; Jia, C.; Liu, W. F.; Cai, W. L.; Yao, L. Z.; Li, X. G. *J. Phys. Chem. B* **2004**, *108*, 1844−1847.
(8) Li, L.; Yang, Y. W.; Huang, X. H.; Li, G. H.; Zhang, L. D. *Nanotechnology* **2006**, *17*, 1706−1712.
(9) Menke, E. J.; Li, Q.; Penner, R. M. *Nano Lett.* **2004**, *4*, 2009−2014.
(10) Menke, E. J.; Brown, M. A.; Li, Q.; Hemminger, J. C.; Penner, R. M. *Langmuir* **2006**, *22*, 10564−10574.
(11) Sapp, S. A.; Lakshmi, B. B.; Martin, C. R. *Adv. Mater.* **1999**, *11*, 402−404.
(12) Wang, W. L.; Wan, C. C.; Wang, Y. Y. *J. Phys. Chem. B* **2006**, *110*, 12974−12980.
(13) Dresselhaus, M. S.; Dresselhaus, G.; Sun, X.; Zhang, Z.; Cronin, S. B.; Koga, T. *Phys. Solid State* **1999**, *41*, 679−682.
(14) Hicks, L. D.; Dresselhaus, M. S. *Phys. Rev. B* **1993**, *47*, 16631−16634.

(15) Huczko, A. *Appl. Phys. A: Mater. Sci. Process.* **2000**, *70*, 365−376.
(16) Prieto, A. L.; Sander, M. S.; Martin-Gonzalez, M. S.; Gronsky, R.; Sands, T.; Stacy, A. M. *J. Am. Chem. Soc.* **2001**, *123*, 7160−7161.
(17) Masuda, H.; Fukuda, K. *Science* **1995**, *268*, 1466−1468.
(18) Sander, M. S.; Prieto, A. L.; Gronsky, R.; Sands, T.; Stacy, A. M. *Adv. Mater.* **2002**, *14*, 665−667.
(19) Sander, M. S.; Gronsky, R.; Sands, T.; Stacy, A. M. *Chem. Mater.* **2003**, *15*, 335−339.
(20) ASM Materials Information. http://products.asminternational.org/hbk/index/jsp, 2006.

NL070711W